

Modelling Based Analysis and Optimization of Simultaneous Saccharification and Fermentation for the Production of Lignocellulosic-Based Xylitol

Ibnu Maulana Hidayatullah

Dept. of Chemical Engineering, Institut Teknologi Bandung

Tjandra Setiadi

Dept. of Chemical Engineering, Insitut Teknologi Bandung

Made Tri Ari Penia Kresnowati (✉ kresnowati@che.itb.ac.id)

Institut Teknologi Bandung <https://orcid.org/0000-0002-8079-4677>

Research

Keywords: lignocellulose, modelling, simultaneous saccharification and fermentation, xylitol

Posted Date: May 11th, 2021

DOI: <https://doi.org/10.21203/rs.3.rs-497052/v1>

License:  This work is licensed under a Creative Commons Attribution 4.0 International License.

[Read Full License](#)

1 **Modelling Based Analysis and Optimization of Simultaneous**
2 **Saccharification and Fermentation for the Production of**
3 **Lignocellulosic-Based Xylitol**

4
5 **I.M. Hidayatullah¹ (0000-0003-4412-2547), T. Setiadi¹ (0000-0003-1850-4680), and M.T.A.P. Kresnowati^{1,2}**
6 **(0000-0002-8079-4677)**

7 ¹Department of Chemical Engineering, Faculty of Industrial Technology, Institut Teknologi Bandung, Jalan
8 Ganesha No. 10, Bandung, West Java, Indonesia, 40132

9 ²Department of Food Engineering, Faculty of Industrial Technology, Institut Teknologi Bandung, Kampus
10 Jatinangor, Sumedang, Indonesia

11 **Corresponding Author: M.T.A.P. Kresnowati (kresnowati@che.itb.ac.id)**

12
13 **Abstract.**

14 Simultaneous saccharification and fermentation (SSF) configuration offers an efficient used of the reactor. In this
15 configuration, both the hydrolysis and fermentation processes are conducted simultaneously in a single bioreactor
16 and the overall process may be accelerated. Problems may arise if both processes have different optimum
17 conditions, and therefore process optimization is required. This paper presents the development of mathematical
18 model over SSF strategy implementation for producing xylitol from hemicellulose component of lignocellulosic
19 materials. The model comprises of the hydrolysis of hemicellulose and the fermentation of hydrolysate into
20 xylitol. The model was simulated for various process temperature, prior hydrolysis time, and inoculum
21 concentration. Simulation of the developed kinetics model shows that the optimum SSF temperature is 36°C,
22 whereas conducting a prior hydrolysis at its optimum hydrolysis temperature will further shorten the processing
23 time and increase the xylitol productivity. On the other hand, increasing the inoculum size will shorten the
24 processing time further. For an initial xylan concentration of 100 g/L, the best condition is obtained by performing
25 21-hour prior hydrolysis at 60°C, followed by SSF at 36°C by adding 2.0 g/L inoculum, giving 46.27 g/L xylitol
26 within 77 hours of total processing time.

27 **Keyword:** lignocellulose, modelling, simultaneous saccharification and fermentation, xylitol

1 Introduction

2 Xylitol is a pentitol or polyalcohol sugar ($C_5H_{12}O_5$) commonly used in the pharmaceutical sector as a dental
3 remineralizing agent. Xylitol can increase salivation and inhibit the cellular activity of cariogenic organisms, thus
4 reducing plaque, gum swelling, dental erosion, and preventing xerostomia (lack of saliva production) [1–5].
5 Xylitol can be used as a sweetener; it is commonly used in food industries and is categorized as safe for diabetics
6 [6–9]. Other than that, xylitol is used as a building block for ethylene glycol and propylene glycol formation using
7 Ruthenium or copper as the catalyst in hydrogenolysis process [10, 11] and as a building block for 2,3,4,5
8 tetrahydroxypentanoic acid and xylonic acid using diperiodatoargentate (III) and Ru (III) as the catalyst through
9 oxidation [12, 13].

10 Conventionally, xylitol production involves hydrogenation of xylose from lignocellulosic biomass.
11 Lignocellulose-based materials are pretreated and hydrolyzed using dilute sulfuric acid, after which the
12 hydrolyzate is purified using chromatography to obtain xylose. Pure xylose solution is then catalytically
13 hydrogenated using Raney-Nickel or Ru/C (Ruthenium-carbon) as the catalysts so that it becomes xylitol [14, 15].
14 This conventional xylitol production method has several disadvantages: the process uses a lot of energy as it is
15 conducted at relatively high pressure and temperature (50–60 bar and 140–200°C); the process requires delicate
16 purification of the hydrolysate to obtain pure xylose; and need more investment in types of equipment,
17 considerable intermediate purification, product recovery, catalyst deactivation, and recycling process [15–17]. An
18 alternative method of producing xylitol from lignocellulose-based materials involves a bioprocessing system that
19 includes enzymatic hydrolysis using xylanase to obtain xylose containing hydrolysate, and microbial fermentation
20 to convert xylose in hydrolysate into xylitol [16, 18, 19]. The hydrolysis and fermentation processes are normally
21 conducted in different reactors or better known as separate hydrolysis and fermentation (SHF) because they have
22 different operating conditions. As a result, the fermentative sugar production process requires a long processing
23 time and is still considered uneconomical.

24 Alternatively, the bioprocess route for xylitol production, that is the hydrolysis and the fermentation, can be
25 conducted simultaneously or better known as simultaneous saccharification and fermentation (SSF). In principle,
26 both the hydrolysis and fermentation processes take place simultaneously in the same reactor, providing direct
27 utilization of hydrolysis product, that is the monomeric sugar, as the carbon source for the fermenting agent form
28 the desired product [19–21]. Consequently, both processes are conducted at the same operating condition.
29 Moreover, the application SSF process from lignocellulose-based materials minimizes the potential substrate

1 inhibition on the fermentation process as well as the potential product inhibition on the enzymatic hydrolysis
2 process, increases the yield and productivity [21–23].

3 Previous studies showed that the use of SSF combined with prior hydrolysis in ethanol production was able to
4 increase the ethanol yield than the SSF only [24, 25]. Burhan et al. [19] reported the implementation of SSF for
5 xylitol production from oil palm empty fruit bunch (OPEFB). In his research, the duration of the prior hydrolysis
6 process was varied to achieve the optimum results. Overall, at the same total processing time, up to 4-fold increase
7 of the xylitol yield from OPEFB when compared with that of SHF was obtained [19]. Prior hydrolysis is necessary
8 to provide sufficient substrate for initializing the fermentation. However, the optimum temperature for conducting
9 both hydrolysis and fermentation simultaneously has been overlooked, the SSF was conducted at the optimum
10 fermentation temperature that led to low enzymatic-hydrolysis activity. The optimum temperature of xylan
11 hydrolysis using xylanase is reported in the range of 40–70°C [26, 27], whereas the optimum temperature for
12 xylitol-producing yeast fermentation is reported in the range of 10–44°C [28–31]. Conducting the SSF at the
13 optimum temperature for both hydrolysis and fermentation would significantly increase the process performance.
14 Followingly the temperature setting for SSF as well as the duration of the prior hydrolysis process can be
15 optimized further to higher xylitol productivity.

16 Modelling may serve as a useful tool to explore the interaction of between parameters. In particular kinetic
17 modelling can be applied to search for the optimal SSF configuration, that is the operating temperature, the
18 duration of the prior hydrolysis or the initialization of the fermentation based on certain initial cell concentration.
19 This paper presents the development of a kinetic model for lignocellulosic material-based xylitol production using
20 SSF. The model was further used for thoroughly studying the effect of process temperature, prior hydrolysis and
21 switching time (the start of SSF) as well as the inoculum size to estimate xylitol concentration and its productivity
22 so that the results could feasibly be applied on a laboratory level and eventually developed on both a pilot and an
23 industrial-scale.

24

25 **Methodology**

26 The model was built by assuming that the process took place in a single batch reactor. The xylan-based
27 hemicellulose in lignocellulosic material was pretreated before being put into the reactor for enzymatic hydrolysis
28 and fermentation. Xylitol production through the bioprocessing pathway is shown in **Fig 1**. During the hydrolysis
29 process, xylan was hydrolysed into xylose. During the fermentation process, xylose was further utilized by the

1 yeast as the carbon sources for biomass growth and xylitol formation. In this model it was assumed that xylitol
 2 was the only metabolite product that was produced during the fermentation and that a decrease in cell
 3 concentration was neglected. Overall, the mass balances describing the process are presented in Eq. 1 – 4.

$$\frac{dC_{xylan}}{dt} = -r_{hyd} \quad (1)$$

$$\frac{dC_{xylose}}{dt} = 1.14 \times r_{hyd} Y_{C_{xylose}/C_{xylan}} - r_{biomass} \frac{1}{Y_{X}/C_{xylose}} \quad (2)$$

$$\frac{dC_X}{dt} = r_{biomass} \quad (3)$$

$$\frac{dC_{Xylitol}}{dt} = r_{xylitol} \quad (4)$$

4

5 Kinetic Model Developments

6 Xylan hydrolysis

7 The rate of hydrolysis process (r_{hyd}) was modelled using the Michaelis Menten reaction kinetics equation as
 8 presented in Eq. 5, with $r_{max,hyd}$ (g/(L.h)) is the maximum rate of hydrolysis, C_{xylan} is the concentration of xylan
 9 (g/L), and $K_{m,hyd}$ is the Michaelis constant for the xylan hydrolysis (g/L) [13].

$$r_{hyd} = \frac{r_{max,hyd} \times C_{xylan}}{K_{m,hyd} + C_{xylan}} \quad (5)$$

10 Like other chemical reactions, a higher temperature can increase the rate of enzymatic reactions. However, higher
 11 temperature also raises the rate of thermal denaturation and the loss of the biocatalyst activity [32, 33]. Within the
 12 range of 40-60°C, however, the overall rate of xylan hydrolysis using xylanase is still increasing with temperature
 13 [26] and the overall effect of temperature on this enzymatic reaction can be modelled following the Arrhenius
 14 equation as is presented in Eq. 7.

$$r_{max,hyd} = k_{hyd} \times E_0 \quad (6)$$

$$k_{hyd} = A_{hyd} \times e^{-\frac{E_{a,hyd}}{RT_{hyd}}} \quad (7)$$

15 E_0 is the concentration of the initial concentration of enzyme used (g/L), k_{hyd} is the catalytic constant of
 16 hydrolysis (h^{-1}), A_{hyd} is the Arrhenius constant for the hydrolysis reaction (h^{-1}), $E_{a,hyd}$ is the activation energy
 17 of the hydrolysis reaction (kJ/mol), R is the universal gas constant (kJ/mol.K), and T_{hyd} is the temperature of
 18 hydrolysis (K).

1 **Biomass growth**

2 The rate of biomass growth is defined following the first order reaction kinetics with respect to the biomass
3 concentration (C_X , g/L) (Eq. 8), whereas the biomass specific growth rate (μ , h^{-1}) is defined following the Monod
4 equation that correlates the the specific growth rate with substrate (xylose) concentration (C_{xylose} , g/L).

$$r_{biomass} = \mu \times C_X \quad (8)$$

$$\mu = \frac{\mu_{max,fer} \times C_{xylose}}{K_{s,fer} + C_{xylose}} \quad (9)$$

5 In which $K_{s,fer}$ is the growth saturation constant on xylose (g/L) and $\mu_{max,fer}$ is the maximum specific growth
6 rate of the fermentation process (h^{-1}). Further, the effect of temperature of biomass growth can be modelled
7 following Sánchez et al. [29] as:

$$\mu_{max,fer} = A_{fer} \times e^{-\frac{E_{g,fer}}{RT}} - B_{fer} \times e^{-\frac{E_{d,fer}}{RT}} \quad (10)$$

8 Where $E_{g,fer}$ is the cell activation energy for growth (kJ/mol), $E_{d,fer}$ is the deactivation energy when the cell has
9 entered the death phase (kJ/mol), A_{fer} is the cell activation coefficient (h^{-1}), B_{fer} is the cell inactivation
10 coefficient (h^{-1}). Other effects of microenvironment conditions, such as the oxygen concentration in the
11 fermentation broth or the acidity level of the media, were not considered in this model. Combination of equations
12 (8), (9), and (10) are given as follows:

$$r_{biomass} = \left(\frac{\left(A_{fer} \times e^{-\frac{E_{g,fer}}{RT}} - B_{fer} \times e^{-\frac{E_{d,fer}}{RT}} \right) \times C_{xylose}}{K_{s,fer} + C_{xylose}} \right) \times C_X \quad (11)$$

13 **Xylitol formation**

Xylitol production rate is modelled using the growth-associated product. The equation is approached as follows
[32]:

$$r_{xylitol} = \mu \times C_X \times Y_{C_{xylitol}/X} \quad (12)$$

Combination of equations (9), (10), and (12) are given as follows.

$$r_{xylitol} = \left(\frac{\left(A \times e^{-\frac{E_g}{RT}} - B \times e^{-\frac{E_d}{RT}} \right) \times C_{xylose}}{K_s + C_{xylose}} \right) \times C_X \times Y_{C_{xylitol}/X} \quad (13)$$

Where $Y_{C_{xylitol}/X}$ is the yield of xylitol formed from biomass activity.

1 **Determination of cell and xylitol productivity**

2 After the xylose was completely converted, we could measure how much cell and xylitol productivity obtained in
3 each configuration process. The cell productivity is determined as follows (Eq. 14).

$$Q_x = \frac{C_x}{t_p} \quad (14)$$

4 Where Q_x and t_p are cell productivity (g/(L.h)) and total processing time (h), respectively. Also, xylitol
5 productivity is defined as follows:

$$Q_{xylitol} = \frac{C_{xylitol}}{t_p} \quad (15)$$

6 Where Q_x is the xylitol productivity (g/(L.h)).

7

8 **Model Simulation and Boundary Condition**

9 The simulation started with the hydrolysis of xylan to xylose followed by the fermentation of the xylose to xylitol.
10 The initial concentration of xylan was set at 100 g/L. Unless stated otherwise, the initial biomass concentration of
11 0.5 g/L was introduced at the beginning of the fermentation process. The maximal total process time was set to
12 be 200 hours.

13 All simulation processes were stopped when the xylitol reached the maximum concentration in each process and
14 the other compounds were considered not to interfere with the process. Particularly for Separate Hydrolysis and
15 Fermentation (SHF), hydrolysis was halted if 1% of xylan residue was obtained. During hydrolysis, the xylobiose
16 and other xylooligosaccharide formation were neglected. Moreover, the xylitol was assumed not consumed by
17 cells or converted into the other compounds so that xylitol accumulation has decreased. The simulations were
18 conducted using the Matlab R2018a. The supporting data for simulations are shown in **Table 1**.

19

20

1 **Results and discussion**

2 **Mapping the effects of temperature on hydrolysis and fermentation**

3 Literature study indicated that the hydrolysis of xylan and the fermentation for xylitol production occurred in
4 different temperature range. For example, Mardawati et al. [26] and Meilany et al. [27] reported the optimum
5 temperature for xylan hydrolysis for obtaining the highest xylose yield at 60°C, whereas Pappu and Gummadi
6 [37] and Sánchez, et al. [29] reported the optimum temperature for fermentation at 35°C. Indeed, previous study
7 showed that the range temperature for the high biomass growth and xylitol productivity was 30-35°C [19, 31, 38].
8 Burhan et al. [19] reported a decrease in fermentation xylitol performance when the temperature was increased
9 from 30 to 37°C. The mapping of the effects of temperature on hydrolysis and fermentation, in particular the
10 maximum rate of hydrolysis (k_{hyd}) and the maximum specific growth rate of biomass (μ_{max}), in the temperature
11 range of 25-60°C are presented in **Fig 2**.

12 Within the temperature range of 25–60°C, the xylan hydrolysis rate was shown to increase along with an increase
13 in temperature, whereas three distinct trends of fermentation rate were observed. An increasing trend of the
14 maximum specific biomass growth rate was observed between 25–34°C. Between 34°C and 42°C, a decreasing
15 trend of the maximum specific biomass growth rate was observed. The biomass could not grow above 42°C. The
16 optimum condition for both hydrolysis and fermentation were expected to be in the range of 25–42°C, in this
17 condition both fermentation and hydrolysis can proceed, although not in each optimum condition.

18

19 **Separate hydrolysis-fermentation (SHF)**

20 Xylitol production via the SHF system was simulated as the reference. The SHF was conducted at the optimum
21 temperature for each process, as have been calculated in the previous section (Fig 2). During this simulation, the
22 hydrolysis was set to proceed at 60°C whereas the following fermentation was set to proceed at 34°C. The
23 temperature switch was assumed to occur instantly. Fermentation was initiated shortly after the completion of
24 xylan hydrolysis, that was at 99% xylan conversion. The results of the simulation of xylitol production using the
25 SHF method are shown in **Fig 3**.

26 **Fig 3** shows that at 48 hours, 99% of xylan has been converted, giving the xylose concentration of 112.68 g/L and
27 a residual xylan of 1.16 g/L. The fermentation was then initiated at that time and the simulation was continued
28 until total processing time of 200 hours. Xylose was consumed slowly by the biomass for the first 32 hours of

1 fermentation. At that time, the biomass was in the lag phase and xylitol was formed slowly. After 80 hours of
2 processing time, fast decrease in xylose concentration was observed, indicating high consumption of xylose for
3 growth and xylitol production. The final concentration of biomass and xylitol that were obtained in the simulation
4 were 21.85 g/L and 46.07 g/L, successively, which were achieved at the 6th days or 128 hours of processing time.
5 Dominguez et al. [38] reported that the xylitol production using 120 g/L synthetic substrate by using 1.2 g/L initial
6 yeast concentration gave xylitol and yeast concentration near to 80 g/L and 5 g/L, respectively, after 72-hour
7 fermentation. The fermentation was conducted at the optimal fermentation temperature and all xylose were
8 utilized within the observed fermentation time. This reported fermentation time was comparable to the time
9 required for consuming all xylose in the fermentation simulation, 80 hours (**Fig 3**).

11 **Simultaneous saccharification and fermentation (SSF)**

12 During SSF, all components of the process: xylan as the substrate, the xylanolytic enzyme, and the biomass
13 inoculum (as the fermenting agent) were present in the bioreactor, such that the hydrolysis and fermentation
14 occurred simultaneously. Two distinct strategies were evaluated: conducting SSF at the optimum hydrolysis
15 temperature (60°C) and conducting the SSF at the optimum fermentation temperature (34°C). The simulation
16 results are presented in **Fig 4**.

17 At the optimum hydrolysis temperature of 60°C (**Fig 4a**), xylan was converted into xylose resulting an increasing
18 xylose profile until 48-hours. The following fermentation, however, could not proceed as the fermenting agent of
19 xylitol production (such as *Debaromyces hansenii*, *Debaromyces nepalensis*, *Pachysolen tannophilus*, or *Candida*
20 *tropicalis*) could only grow in the temperature range of 15-40°C [29–31, 39, 40]. Thereby no biomass growth nor
21 product formation is observed (**Fig 2**). By the end of this simulation, only as much as 115.31 g/L of xylose was
22 formed.

23 At the optimum fermentation temperature of 34°C (**Fig 4b**), hydrolysis proceeded slowly. Xylan was slowly
24 hydrolyzed and would be completely hydrolyzed at 110 hours. Although the biomass inoculum was already
25 present from the start of SSF, the low xylose concentration led to slow biomass growth. Significant biomass
26 concentration was only observed after 43 hours and the biomass reached stationary phase when the substrate
27 exhausted. Xylose was completely utilized at 109 hours, resulting in xylitol and biomass concentration of 46.06
28 g/L and 21.83 g/L, respectively. Nevertheless, in comparison to the SHF process, the SSF method proceeded faster
29 to achieve the same xylitol concentration. Applying the fermentation optimum temperature is preferable than the
30 optimum hydrolysis temperature in SSF.

1

2 **Simultaneous hydrolysis-fermentation at optimum SSF temperature**

3 In determining the optimum temperature for SSF, simulations were conducted within the temperature range of
4 30-43°C using Eq. 7, Eq. 11, and Eq. 13 for temperature-dependent hydrolysis, biomass growth, and xylitol
5 formation, respectively. **Fig 5** showed the contour plot between temperature, the processing time, and the resulting
6 xylitol productivity. The lowest to the highest xylitol productivity was represented by the dark blue to dark red
7 contour area, respectively.

8 The maximum xylitol concentration can always be achieved at various SSF temperature. However, the processing
9 time required to achieve the maximum xylitol concentration varied with temperature, leading to a variation in the
10 xylitol productivity. The low enzymatic activity at the range of temperature of 30-43°C resulted in slow xylose
11 accumulation. The low xylose concentration led to slow biomass growth and xylitol formation. For total
12 processing time under 60 hours, low xylitol productivity ($< 0,15$ g/(L.h)) was observed at the simulated
13 temperature range (**Fig 5**). An increasing trend of xylitol productivity was observed at processing time 60-100
14 hours. However, the xylitol productivity slowly decreased after 100 hours of processing time. The optimum xylitol
15 productivity was achieved in the temperature range of 34-37°C, marked by the dark red region in **Fig 5**. At 36°C
16 the maximum xylitol concentration was achieved at 102 hours, gave the highest xylitol productivity of 0.45
17 g/(L.h). Conducting SSF at this optimum SSF temperature, 36°C, led to higher xylitol productivity compared to
18 conducting SSF at the optimum fermentation temperature.

19 Previous research on SSF for xylitol production from OPEFB that was conducted at 30°C with initial xylan
20 concentration of 10 g/L (assuming the average xylan composition in OPEFB was 22.5% [41]) for 120 hours, gave
21 xylitol productivity of 0.047 g/L [19]. Compared to this, this ideal simulation showed faster processing time and
22 resulted in higher xylitol productivity.

23

24 **Semi-simultaneous hydrolysis-fermentation and the effect of initial cell concentration**

25 The performance of SSF may be improved by conducting a prior hydrolysis process, at the optimized temperature
26 for hydrolysis, before the initiation of SSF. The overall process, the combination of the prior hydrolysis process
27 and the SSF process is called as semi-simultaneous hydrolysis and fermentation (semi-SSF). In practice the
28 initiation of SSF can be set by the addition of biomass inoculum on various concentration. This event will be
29 referred as the switching time, in the remaining discussion.

1 The determination of the optimum switching time was conducted by varying the duration of prior hydrolysis,
2 ranging between 0 to 48 hours, at certain initial cell concentration. The results are shown in **Fig 6**, with the dark
3 blue to dark red colour denotes the lowest to highest xylitol concentration, respectively.

4 In general, an increase in the switching time resulted in longer total processing time required to achieve the
5 maximum xylitol concentration (**Fig 6**). The best configuration was obtained by prior hydrolysis time of 8 hours
6 led to total processing time of 93 hours to achieve the maximum xylitol concentration (**Fig 6a**). The later the
7 switching time, the lower the ability of the biomass to ferment so that productivity decreases. The obtained results
8 are consistent with previous study conducted by Burhan et al. [15], in which prior hydrolysis resulted in higher
9 xylitol concentration and productivity.

10 The overall processing time could be further improved by increasing the initial biomass concentration for the
11 fermentation, or in other words increasing the inoculum size added to the system (**Fig 6b-c**). **Table 2** shows the
12 effects of initial cell concentrations on cell and xylitol productivities. In addition, the increase in the initial cell
13 concentrations shortened the total processing time despite of longer prior hydrolysis time. These results showed
14 that the fermentation process was the limiting factor of xylitol production. Increasing concentration of cell
15 inoculum is thus recommended to increase xylitol productivity and shorten the total process time.

16

17 **Comparison of configurations of all processes**

18 Various process configurations for xylitol production have been simulated. We summarized the effect of process
19 configuration and process temperature to overall processing time, cell and xylitol productivities at the same initial
20 xylan and cell concentration (100 g/L and 0.5 g/L). The summary of cell and xylitol productivity and the time
21 required to achieve the maximum xylitol concentration are shown in **Table 3**. SSF at optimum condition
22 temperature provided better cell and xylitol productivities than SSF at the optimum fermentation temperature.
23 SSF with high initial cell concentration increased the cell and xylitol productivities further. The best SSF
24 configuration obtained in the simulations, that was 21 hours prior hydrolysis at the optimum hydrolysis
25 temperature followed by SSF at 36°C by adding cell inoculum up to 2 g/L, shortened the overall processing time
26 to achieve the maximum xylitol concentration to 77 hours, or 39.84%, when compared with the SHF. The overall
27 processing time for SHF was 128 hours whereas the overall processing time for the best SSF configuration was
28 77 hours.

1 The obtained results confirmed previous results of Burhan et al. [19] and Öhgren et al. [42] which produced xylitol
2 and ethanol using the SHF and SSF methods and obtained higher productivity results when using the SSF
3 configuration.

4 The results of SSF simulation showed that the optimum temperature, intermediate xylose formation-reduction,
5 xylitol formed, and biomass growth could be predicted adequately. Experimental validation through testing the
6 SSF temperature and the pre-hydrolysis time could be conducted further to confirm the accuracy of model
7 parameters that were used.

8 Overall, simulation of the developed kinetic model has been applied to design the configuration and the
9 operational of SSF process. The model could be further improved by the incorporation of non-ideal conditions
10 such as the inhibitory term to the hydrolysis process [43] or the inhibitory term to xylitol fermentation process [7,
11 44, 45] to give a more accurate estimation of the SSF process of lignocellulosic material. Details kinetics of the
12 related process as well as the estimated concentration of inhibitory substance in a specific process, for example
13 SSF of OPEFB, needed to be defined. Nonetheless, this paper showed that SSF or semi SSF is an alternative
14 process configuration that led to higher product (xylitol) productivity.

15

16 **Concluding Remarks**

17 The kinetic model describing the SSF for xylitol production from hemicellulose of lignocellulosic material has
18 been successfully developed and simulated. Our simulation showed that the performance of SSF process was
19 affected by the process temperature, the length of prior hydrolysis or the switching time, and the biomass initial
20 concentration. Overall, it was concluded that the SSF configuration led to higher xylitol productivity than the
21 SHF. The best SSF configuration was combination of prior hydrolysis at the optimum hydrolysis temperature for
22 21 hour (semi SSF), SSF temperature of 36°C, and initial biomass concentration of 2 g/L, which the led to an
23 increase cell and xylitol productivity to 0.307 and 0.599 g/(L.h), respectively.

24

25 **Declarations**

26 **Ethics approval and consent to participate**

27 Not applicable

28

29 **Consent for publication**

1 All authors confirm and consent to publish this manuscript.

2

3 **Availability of data and materials**

4 The simulation data that support the findings of this study are available from the corresponding author upon
5 reasonable request.

6

7 **Competing interest**

8 The authors declare that they have no conflict of interest.

9

10 **Funding**

11 This research was funded by the Ministry of Research and Technology (Kemenristekdikti) Republik Indonesia
12 under the Program Magister Doktor untuk Sarjana Unggul (PMDSU) (grant numbers 0017y/I1.C06/PL/2019).

13

14 **Authors' contributions**

15 IMH: Conceptualization, Data acquisition, Formal analysis, Investigation, Visualization, Writing-original draft,
16 Writing-review and editing; TS: Conceptualization, Funding acquisition, Methodology, Project administration,
17 Supervision; MTAPK: Conceptualization, Formal analysis, Methodology, Project administration, Supervision,
18 Visualization, Writing-original draft, Writing-review and editing.

19

20 **Acknowledgments**

21 We would like to acknowledge the Ministry of Research and Technology (Kemenristekdikti) Republik Indonesia
22 under the Program Magister Doktor untuk Sarjana Unggul (PMDSU) for research funding support (grant numbers
23 0017y/I1.C06/PL/2019). Also, we would like to thank Aulia Maulana for assisting in the model and simulation.

24

25 **Authors' information**

26 ¹Department of Chemical Engineering, Faculty of Industrial Technology, Institut Teknologi Bandung, Jalan
27 Ganesha No. 10, Bandung, West Java, Indonesia, 40132. ²Department of Food Engineering, Faculty of Industrial
28 Technology, Institut Teknologi Bandung, Kampus Jatinangor, Sumedang, Indonesia.

29

1 **References**

- 2 1. Nayak PA, Nayak UA, Khandelwal V (2014) The effect of xylitol on dental caries and oral flora. *Clin*
3 *Cosmet Investig Dent* 6:89–94. <https://doi.org/10.2147/CCIDE.S55761>
- 4 2. Mäkinen KK (2010) Sugar Alcohols, Caries Incidence, and Remineralization of Caries Lesions: A
5 Literature Review. *Int J Dent* 2010:1–23. <https://doi.org/10.1155/2010/981072>
- 6 3. Ramesh S, Muthuvelayudham R, Rajesh Kannan R, Viruthagiri T (2013) Enhanced production of
7 xylitol from corncob by *Pachysolen tannophilus* using response surface methodology. *Int J Food Sci*
8 2013:. <https://doi.org/10.1155/2013/514676>
- 9 4. Granstrom TB (2002) Biotechnological production of xylitol with *Candida* yeasts
- 10 5. Aranda-Barradas JS, Garibay-Orijel C, Badillo-Corona JA, Salgado-Manjarrez E (2010) A
11 stoichiometric analysis of biological xylitol production. *Biochem Eng J* 50:1–9.
12 <https://doi.org/10.1016/j.bej.2009.10.023>
- 13 6. Ur-Rehman S, Mushtaq Z, Zahoor T, et al (2015) Xylitol: A Review on Bioproduction, Application,
14 Health Benefits, and Related Safety Issues. *Crit Rev Food Sci Nutr* 55:1514–1528.
15 <https://doi.org/10.1080/10408398.2012.702288>
- 16 7. Zhang J, Geng A, Yao C, et al (2012) Effects of lignin-derived phenolic compounds on xylitol
17 production and key enzyme activities by a xylose utilizing yeast *Candida athensensis* SB18. *Bioresour*
18 *Technol* 121:369–378. <https://doi.org/10.1016/j.biortech.2012.07.020>
- 19 8. Anil N, Sudarshan K, Naidu NN, Ahmed M (2016) Production of Xylose from Corncobs. *Int J Eng Res*
20 *Appl* 6:77–84
- 21 9. Cortez DV, Roberto IC (2010) Improved xylitol production in media containing phenolic aldehydes:
22 Application of response surfacemethodology for optimization and modeling of bioprocess. *J Chem*
23 *Technol Biotechnol* 85:33–38. <https://doi.org/10.1002/jctb.2265>
- 24 10. Sun J, Liu H (2011) Selective hydrogenolysis of biomass-derived xylitol to ethylene glycol and
25 propylene glycol on supported Ru catalysts. *Green Chem* 13:135–142.
26 <https://doi.org/10.1039/c0gc00571a>
- 27 11. Huang Z, Chen J, Jia Y, et al (2014) Selective hydrogenolysis of xylitol to ethylene glycol and
28 propylene glycol over copper catalysts. *Appl Catal B Environ* 147:377–386.
29 <https://doi.org/10.1016/j.apcatb.2013.09.014>
- 30 12. Gowda JI, Nandibewoor ST (2012) Mechanism of oxidation of xylitol by a new oxidant,

- 1 diperiodatoargentate (III), in aqueous alkaline medium. *Synth React Inorganic, Met Nano-Metal Chem*
2 42:1183–1191. <https://doi.org/10.1080/15533174.2012.684261>
- 3 13. Srivastava A, Bansal S (2015) Kinetics and Mechanism of Ru (III) Catalysed Oxidation of Xylitol by
4 Chloramine-T in Perchloric Acid Medium. 4:39–48
- 5 14. Baudel HM, de Abreu CAM, Zaror CZ (2005) Xylitol production via catalytic hydrogenation of
6 sugarcane bagasse dissolving pulp liquid effluents over Ru/C catalyst. *J Chem Technol Biotechnol*
7 80:230–233. <https://doi.org/10.1002/jctb.1155>
- 8 15. Delgado Arcaño Y, Valmaña García OD, Mandelli D, et al (2020) Xylitol: A review on the progress and
9 challenges of its production by chemical route. *Catal Today* 344:2–14.
10 <https://doi.org/10.1016/j.cattod.2018.07.060>
- 11 16. Rafiqul ISM, Sakinah AMM (2013) Processes for the Production of Xylitol-A Review. *Food Rev Int*
12 29:127–156. <https://doi.org/10.1080/87559129.2012.714434>
- 13 17. Dasgupta D, Bandhu S, Adhikari DK, Ghosh D (2017) Challenges and prospects of xylitol production
14 with whole cell bio-catalysis: A review. *Microbiol Res* 197:9–21.
15 <https://doi.org/10.1016/j.micres.2016.12.012>
- 16 18. Kresnowati M, Mardawati E, Setiadi T (2015) Production of Xylitol from Oil Palm Empty Friuts
17 Bunch: A Case Study on Bio refinery Concept. *Mod Appl Sci* 9:206.
18 <https://doi.org/10.5539/mas.v9n7p206>
- 19 19. Burhan KH, Kresnowati MTAP, Setiadi T (2019) Evaluation of simultaneous saccharification and
20 fermentation of oil palm empty fruit bunches for xylitol production. *Bull Chem React Eng & Catal*
21 14:559–567. <https://doi.org/10.9767/bcrec.14.3.3754.559-567>
- 22 20. Wyman CE, Spindler DD, Grohmann K (1992) Simultaneous saccharification and fermentation of
23 several lignocellulosic feedstocks to fuel ethanol. *Biomass and Bioenergy* 3:301–307.
24 [https://doi.org/10.1016/0961-9534\(92\)90001-7](https://doi.org/10.1016/0961-9534(92)90001-7)
- 25 21. F Alfani, A Gallifuoco, A Saporosi AS and MC (2002) Comparison of SHF and SSF processes for the
26 bioconversion of steam-exploded wheat straw. 123:71–75
- 27 22. Ballesteros M, Oliva JM, Negro MJ, et al (2004) Ethanol from lignocellulosic materials by a
28 simultaneous saccharification and fermentation process (SFS) with *Kluyveromyces marxianus* CECT
29 10875. *Process Biochem* 39:1843–1848. <https://doi.org/10.1016/j.procbio.2003.09.011>
- 30 23. Tomás-Pejó E, Oliva JM, Ballesteros M, Olsson L (2008) Comparison of SHF and SSF processes from

- 1 steam-exploded wheat straw for ethanol production by xylose-fermenting and robust glucose-fermenting
2 *Saccharomyces cerevisiae* strains. *Biotechnol Bioeng* 100:1122–1131. <https://doi.org/10.1002/bit.21849>
- 3 24. Shen J, Agblevor FA (2010) Modeling semi-simultaneous saccharification and fermentation of ethanol
4 production from cellulose. *Biomass and Bioenergy* 34:1098–1107.
5 <https://doi.org/10.1016/j.biombioe.2010.02.014>
- 6 25. Gonçalves FA, Ruiz HA, Nogueira CDC, et al (2014) Comparison of delignified coconuts waste and
7 cactus for fuel-ethanol production by the simultaneous and semi-simultaneous saccharification and
8 fermentation strategies. *Fuel* 131:66–76. <https://doi.org/10.1016/j.fuel.2014.04.021>
- 9 26. Mardawati E, Werner A, Bley T, et al (2014) The Enzymatic Hydrolysis of Oil Palm Empty Fruit
10 Bunches to Xylose. *J Japan Inst Energy* 93:973–978. <https://doi.org/10.3775/jie.93.973>
- 11 27. Meilany D, Mardawati E, Tri M, et al (2017) Kinetic Study of Oil Palm Empty Fruit Bunch Enzymatic
12 Hydrolysis. 17:197–202
- 13 28. Sampaio FC, De Moraes CA, De Faveri D, et al (2006) Influence of temperature and pH on xylitol
14 production from xylose by *Debaryomyces hansenii* UFV-170. *Process Biochem* 41:675–681.
15 <https://doi.org/10.1016/j.procbio.2005.08.019>
- 16 29. Sánchez S, Bravo V, Moya AJ, et al (2004) Influence of temperature on the fermentation of D-xylose by
17 *Pachysolen tannophilus* to produce ethanol and xylitol. *Process Biochem* 39:673–679.
18 [https://doi.org/10.1016/S0032-9592\(03\)00139-0](https://doi.org/10.1016/S0032-9592(03)00139-0)
- 19 30. Gummati SN, Kumar S (2008) Effects of temperature and salts on growth of halotolerant
20 *Debaryomyces nepalensis* NCYC 3413. *Am. J. Food Technol.* 3:354–360
- 21 31. Mohamad NL, Mustapa Kamal SM, Gliew A (2009) Effects of temperature and pH on xylitol recovery
22 from oil palm empty fruit bunch hydrolysate by *Candida tropicalis*. *J. Appl. Sci.* 9:3192–3195
- 23 32. Michael L. Shuler; Fikret Kargi (2002) *Bioprocess Engineering Basic Concepts*, Second. Prentice hall
24 PTR, New Jersey (NJ)
- 25 33. John Villadsen; Jens Nielsen; Gunnar Liden (2011) *Bioreaction Engineering Principles*, Third. Springer,
26 New York
- 27 34. Mardawati E, Trirakhmadi A, Kresnowati M, Setiadi T (2017) Kinetic study on Fermentation of xylose
28 for The Xylitol Production. *J Ind Inf Technol Agric* 1:1. <https://doi.org/10.24198/jiita.v1i1.12214>
- 29 35. Josefa K. M, Alejandro B, Juan P. A, et al (2018) Biotechnological Production of Xylitol from Oil Palm
30 Empty Fruit Bunches Hydrolysate. *Adv J Food Sci Technol* 16:134–137.

- 1 <https://doi.org/10.19026/ajfst.16.5945>
- 2 36. Zhou J, Liu Y, Shen J, et al (2015) Kinetic and thermodynamic characterization of a novel low-
3 temperature-active xylanase from *Arthrobacter* sp. GN16 isolated from the feces of *Grus nigricollis*.
4 *Bioengineered* 6:111–114. <https://doi.org/10.1080/21655979.2014.1004021>
- 5 37. Pappu JSM, Gummadi SN (2016) Modeling and simulation of xylitol production in bioreactor by
6 *Debaryomyces nepalensis* NCYC 3413 using unstructured and artificial neural network models.
7 *Bioresour Technol* 220:490–499. <https://doi.org/10.1016/j.biortech.2016.08.097>
- 8 38. Dominguez J. M. Cheng S. G. 2 and Tsao G. T. (1997) Production of xylitol from D-xylose by
9 *debaryomyces hansenii*. *Appl Biochem Biotechnol - Part A Enzym Eng Biotechnol* 63–65:117–127.
10 <https://doi.org/10.1007/BF02920418>
- 11 39. Breuer U, Harms H (2006) *Debaryomyces hansenii* - An extremophilic yeast with biotechnological
12 potential. *Yeast* 23:415–437. <https://doi.org/10.1002/yea.1374>
- 13 40. Converti A, Perego P, Domínguez JM, Silva SS (2001) Effect of temperature on the microaerophilic
14 metabolism of *Pachysolen tannophilus*. *Enzyme Microb Technol* 28:339–345.
15 [https://doi.org/10.1016/S0141-0229\(00\)00330-6](https://doi.org/10.1016/S0141-0229(00)00330-6)
- 16 41. Bajpai P (2014) Chapter 2 - Xylan: Occurrence and Structure. In: Bajpai P (ed) *Xylanolytic Enzymes*.
17 Academic Press, Amsterdam, pp 9–18
- 18 42. Öhgren K, Bura R, Lesnicki G, et al (2007) A comparison between simultaneous saccharification and
19 fermentation and separate hydrolysis and fermentation using steam-pretreated corn stover. *Process*
20 *Biochem* 42:834–839. <https://doi.org/10.1016/j.procbio.2007.02.003>
- 21 43. Maulana Hidayatullah I, Setiadi T, Tri Ari Penia Kresnowati M, Boopathy R (2020) Xylanase inhibition
22 by the derivatives of lignocellulosic material. *Bioresour Technol* 300:122740.
23 <https://doi.org/10.1016/j.biortech.2020.122740>
- 24 44. Wannawilai S, Chisti Y, Sirisansaneeyakul S (2017) A model of furfural-inhibited growth and xylitol
25 production by *Candida magnoliae* TISTR 5663. *Food Bioprod Process* 105:129–140.
26 <https://doi.org/10.1016/j.fbp.2017.07.002>
- 27 45. Sampaio FC, Torre P, Passos FML, et al (2007) Influence of inhibitory compounds and minor sugars on
28 xylitol production by *Debaryomyces hansenii*. *Appl Biochem Biotechnol* 136:165–181.
29 <https://doi.org/10.1007/BF02686021>
- 30

1 **Figure Captions**

2 **Fig 1.** Bioprocess-based xylitol production

3 **Fig 2.** Effect of temperature on hydrolysis and fermentation processes; the blue line (—) denotes the
4 fermentation model; the red line (—) represents the hydrolysis model

5 **Fig 3.** Xylitol production by using the SHF method, both the hydrolysis and the succeeding fermentation were
6 conducted at their optimum temperatures

7 **Fig 4.** Xylitol production via SSF method conducted at (a) the optimum hydrolysis temperature and (b) the
8 optimum fermentation temperature

9 **Fig 5.** The results of SSF simulation for contour map showing temperature, process time, and xylitol
10 productivity

11 **Fig 6.** Contour map showing the effect of switching time to xylitol concentration at initial cell concentration of
12 (a) 0.5 g/L; (b) 1 g/L; and (c) 2 g/L.

13

14 **Table Captions**

15 **Table 1.** Supporting data for modeling and simulation of xylitol production

16 **Table 2.** The effect of initial cell concentration in the inoculum to SSF for xylitol production

17 **Table 3.** Results of all configurations of processes of xylitol production

Figures

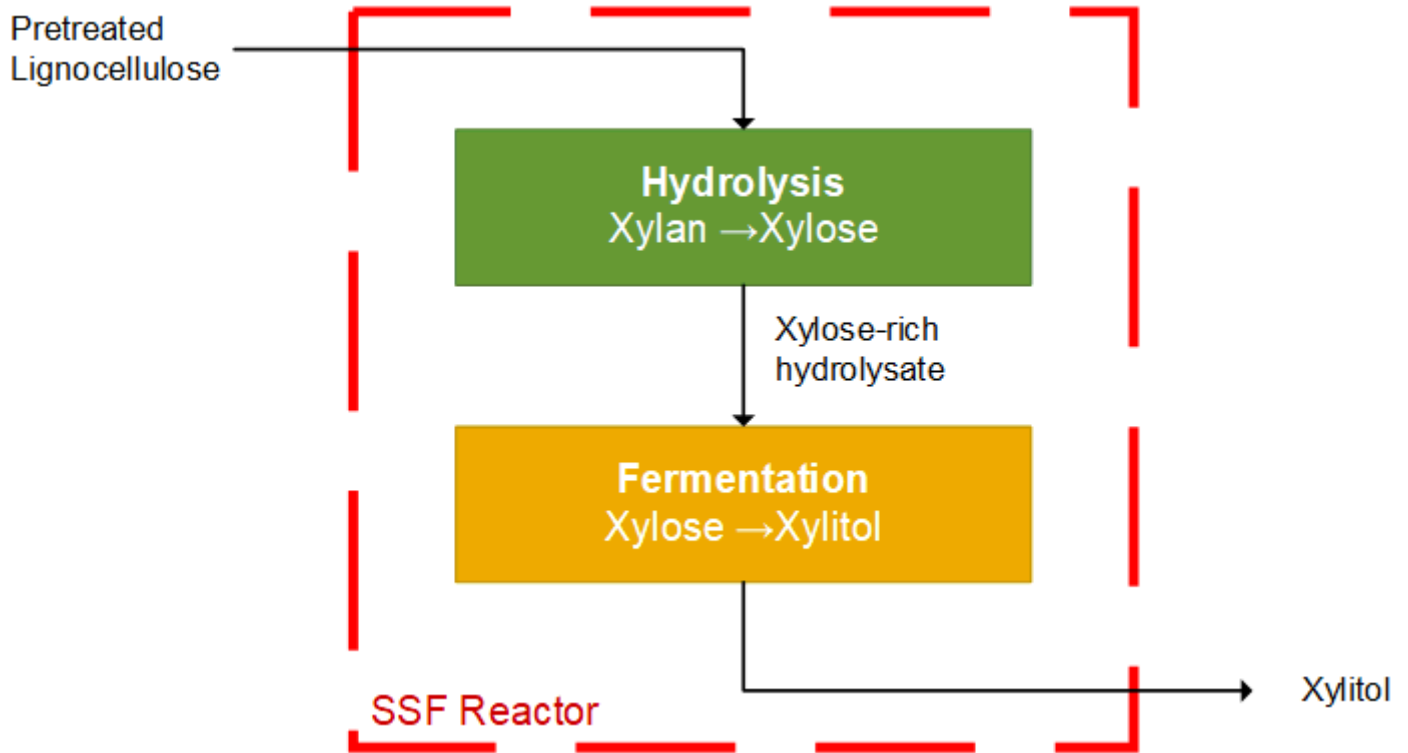


Figure 1

Bioprocess-based xylitol production

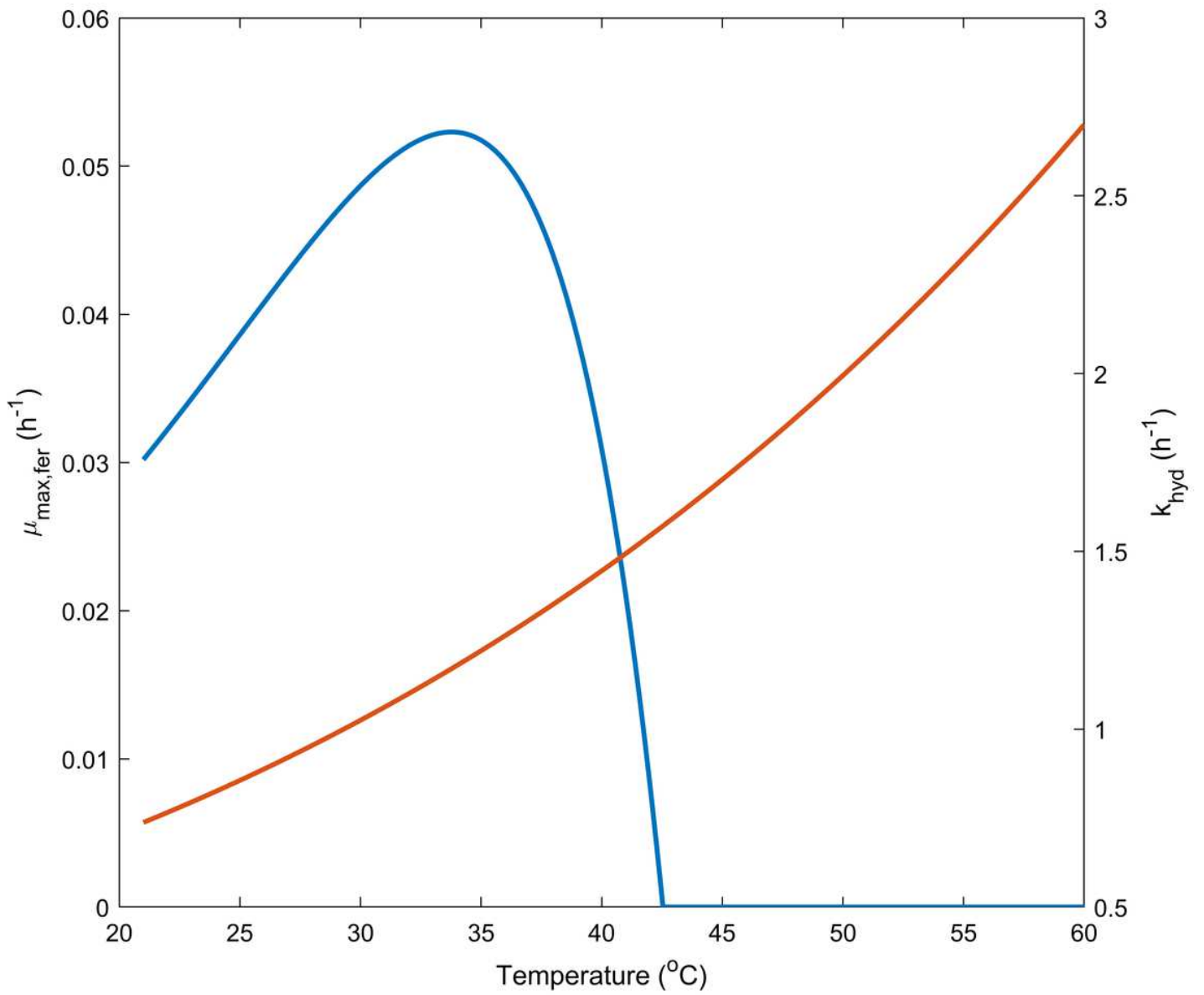


Figure 2

Effect of temperature on hydrolysis and fermentation processes; the blue line (—) denotes the fermentation model; the red line (—) represents the hydrolysis model

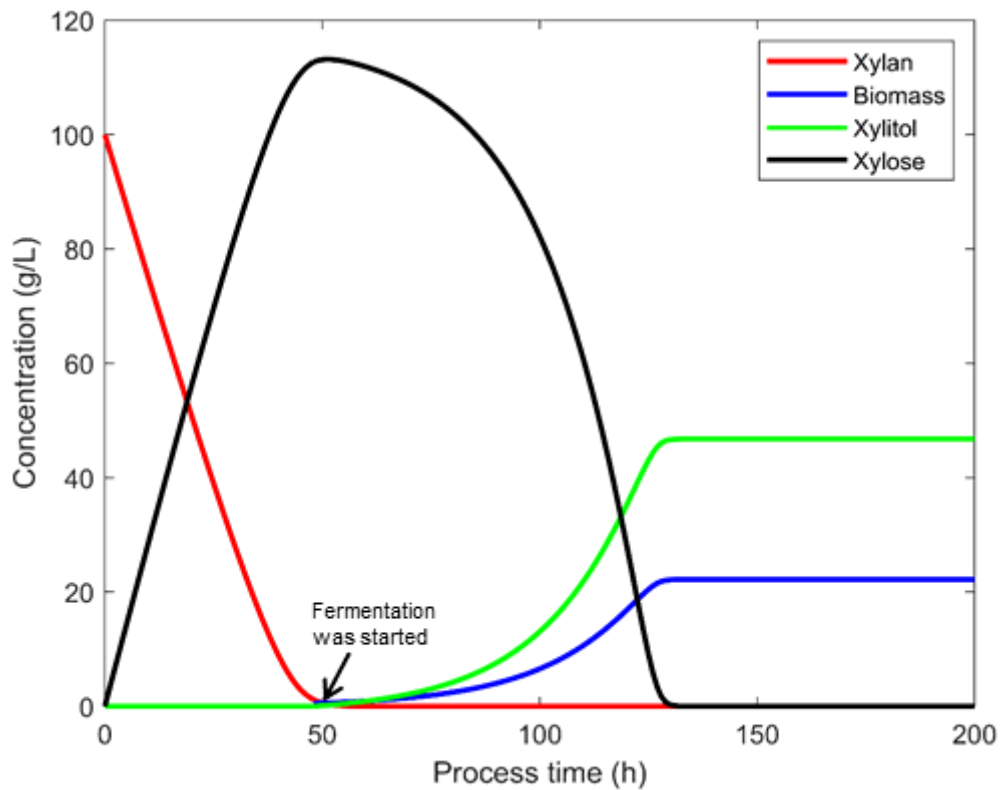


Figure 3

Xylitol production by using the SHF method, both the hydrolysis and the succeeding fermentation were conducted at their optimum temperatures

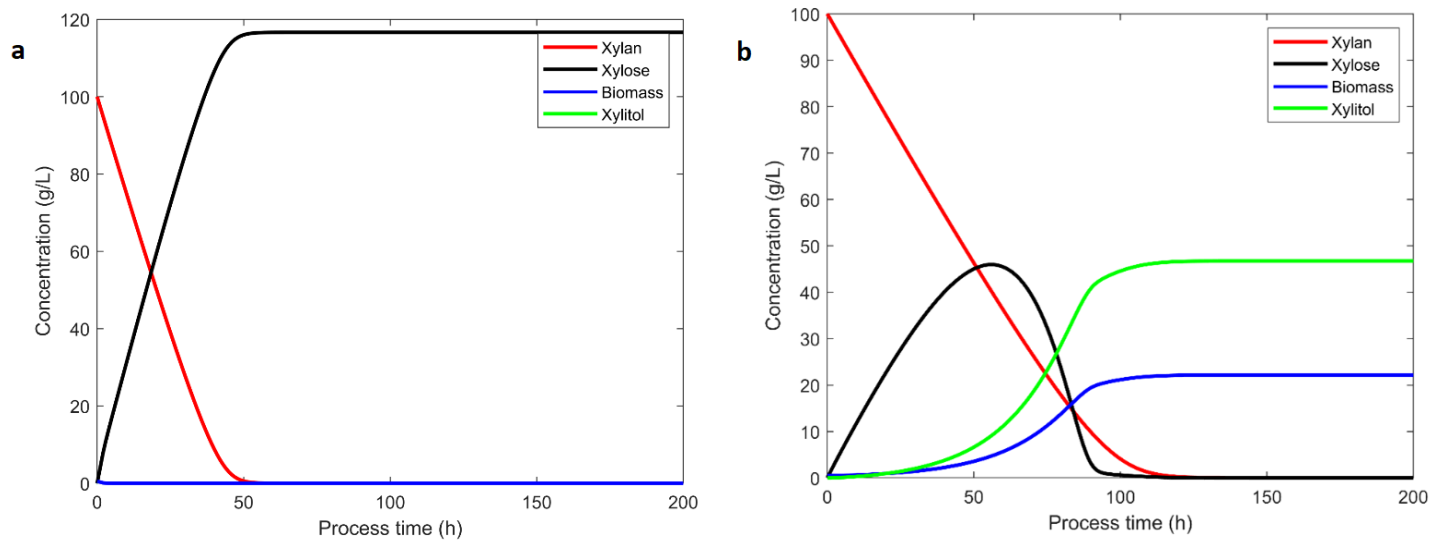


Figure 4

Xylitol production via SSF method conducted at (a) the optimum hydrolysis temperature and (b) the optimum fermentation temperature

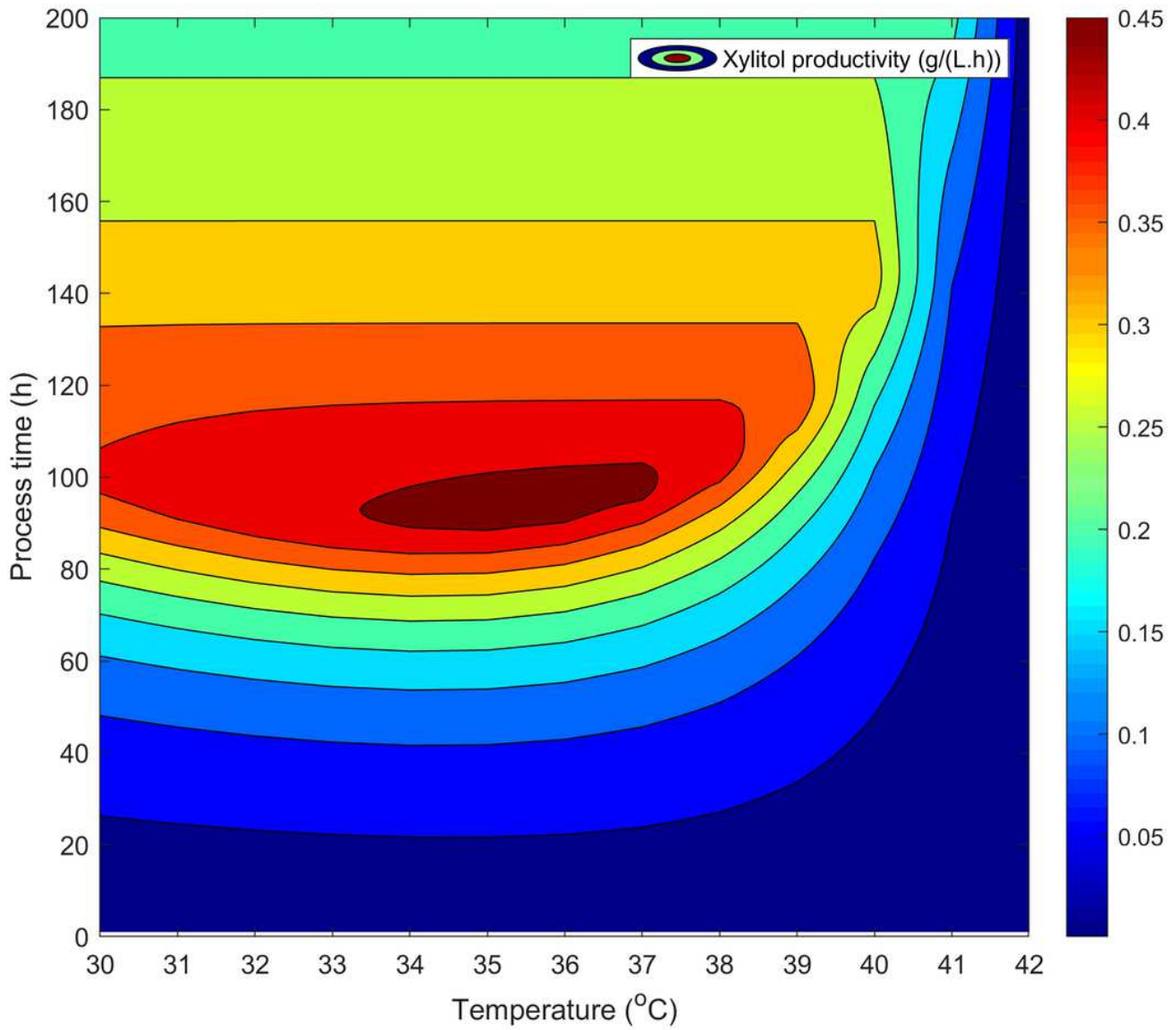


Figure 5

The results of SSF simulation for contour map showing temperature, process time, and xylitol productivity

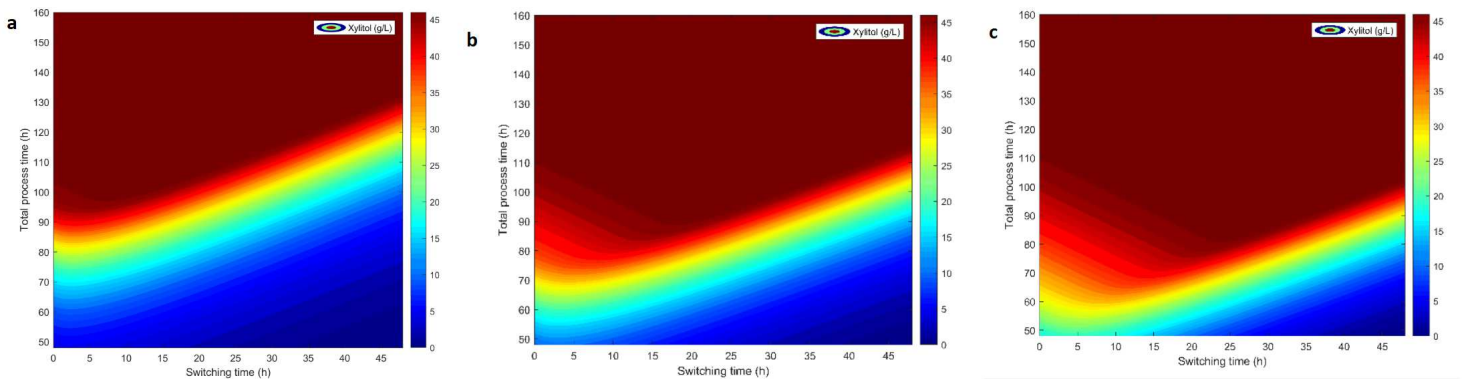


Figure 6

Contour map showing the effect of switching time to xylitol concentration at initial cell concentration of (a) 0.5 g/L; (b) 1 g/L; and (c) 2 g/L.

Supplementary Files

This is a list of supplementary files associated with this preprint. Click to download.

- [GraphicalAbstractSSF.png](#)